TransAT

Handbook Series

理论手册–多相流

Version 5.7.1

Contents

Chapter 1

Interface Tracking Methods

1.1 The general approach

Interface Tracking Methods (ITM) are used for free-surface and interfacial flows which involve two or more immiscible fluids (e.g., liquid-liquid or liquid-gas systems) separated by sharp interfaces which evolve in time. Interface tracking/capturing schemes are methods that are able to locate the interface by capturing the interface by keeping track of the evolution of an appropriate field.

The formulation is based on solving a single set of transport equations for the whole computational domain and treating the two phases as a single fluid with variable material properties. Changes in these properties are taken into account by advecting the phase-indicator function $\chi(x, t)$:

$$\frac{\partial \chi}{\partial t} + u_j^I \frac{\partial \chi}{\partial x_j} = 0 \tag{1.1}$$

where the interface velocity u^I reduces in isothermal flow conditions (no phase change) to the local fluid velocity u.

Mass exchange terms and capillary forces are represented as momentum and energy sources, described as delta functions or smoothed gradients at or across the interface. The mass, momentum and energy balance equations for incompressible interfacial flow are written as

$$\frac{\partial u_j}{\partial x_j} = 0 \tag{1.2}$$

$$\frac{\partial \rho u_i}{\partial t} + \frac{\partial}{\partial x_j}(\rho u_i u_j) = \frac{\partial}{\partial x_j}(-p\delta_{ij} + \sigma_{ij}) + \rho g_i + \gamma \, \kappa \, \delta^I(\phi) \, n_i \tag{1.3}$$

$$\rho \, C_p \frac{\partial T}{\partial t} + \rho \, C_p \, u_j \frac{\partial T}{\partial x_j} = \frac{\partial}{\partial x_j}\left(\lambda \frac{\partial T}{\partial x_j}\right) + \dot{Q}''' \tag{1.4}$$

where γ is the surface tension coefficient, κ is the interface curvature, n is the normal vector to the interface, δ^I is a smoothed Dirac delta function centered at the interface, T is the temperature, C_p is the heat capacity of the fluids, λ is the heat conductivity, and $\dot{Q}$ is the volumetric heat source. Material properties are updated using χ:

$$\rho(\chi, t) = \sum \chi^k \rho^k \tag{1.5}$$

$$\mu(\chi, t) = \sum \chi^k \mu^k \tag{1.6}$$

$$C_p(\chi, t) = \frac{\sum \chi^k \rho^k C_p^k}{\sum \chi^k \rho^k} \tag{1.7}$$

$$\lambda(\chi, t) = \sum \chi^k \lambda^k \tag{1.8}$$

1.2   The VOF methodology

The VOF approach relies on the definition of the *liquid volume-fraction* field occupied by one of the phases within volume V, and is conventionally denoted in a discrete form by F_{ijk}:

$$F_{ijk} = \frac{1}{V_{ijk}} \int_{V_{ijk}} \chi(x, t) dV_{ijk} \tag{1.9}$$

In the VOF context, Eq. (1.1), therefore, represents the evolution of the *liquid volume-fraction*, identifying flow regions containing pure liquid (where $F_{ijk} = 1$) from pure gas flow regions (where $F_{ijk} = 0$). Interfacial cells are such that $0 < F_{ijk} < 1$. The VOF method does not amount solely to the solution of:

$$\frac{\partial F}{\partial t} + u_j \frac{\partial F}{\partial x_j} = 0 \tag{1.10}$$

It requires accurate algorithms for advecting the volume fraction function so as to preserve the thickness of the interface. In order to keep the interface sharp a special advection scheme referred to as the Compressive Interface Capturing Scheme for Arbitrary Meshes (CICSAM) (Ubbink, 1997; Ubbink & Issa, 1999) is used.

1.3   The Level Set method

1.3.1   The scheme

The Level Set approach (Osher & Sethian, 1988) consists in solving a hyperbolic equation:

$$\frac{\partial \phi}{\partial t} + u_j^I \frac{\partial \phi}{\partial x_j} = 0 \tag{1.11}$$

to track the interface on a fixed Eulerian grid, where $\phi(\mathbf{x}, t)$ is a smooth signed-distance function referring to the shortest distance to the front. Negative values correspond to one of the fluids and positive values to the other. The exact location of the interface corresponds to the zero level of ϕ. To update material properties like density, viscosity and thermal conductivity, a Heaviside function $H(\phi)$ is introduced and defined by

$$H(\phi) = \left\{ \begin{array}{ll} 0 & \text{if} \quad \phi < 0 \\ 1 & \text{if} \quad \phi \geq 0 \end{array} \right. \tag{1.12}$$

This implies that ϕ_{ijk} is linked in discrete form to the *liquid volume fraction* field F_{ijk} through

$$F_{ijk} = \frac{1}{V_{ijk}} \int_{V_{ijk}} H\left[\phi_{ijk}\right] dV_{ijk} \tag{1.13}$$

A modified Heaviside function denoted by $\overline{H}(\phi)$ is employed to smooth the physical properties across an interface thickness of 2δ.

$$\rho(\phi, t) = \sum_k \rho^k \, \overline{H}(\phi) \tag{1.14}$$

where $\overline{H}^k(\phi)$ is the modified Heaviside function defined by

$$\overline{H}(\phi) = \frac{1}{2} \left(1 + \tanh\left(\frac{2\phi}{\delta} \right) \right) \tag{1.15}$$

The same modified Heaviside function is concurrently employed to determine the surface tension.

1.3.2   Re-distancing scheme

As numerical errors cause the contours of the Level Set field to deform as the phase moves, a re-distancing algorithm is required to regularise the function: advecting the initial distance function $\phi(\mathbf{x}, 0)$ will not be maintained as such. An extra re-distancing algorithm preserving $|\nabla\phi| = 1$ around the zero level of ϕ is required.

The scheme of Sussman *et al.* (1994) consists of advecting an intermediate equation for a correction field $d(x, t)$ during a period of intermediate time $\tilde{t}$:

$$\frac{\partial d}{\partial \tau} = sgn(d_0)(1 - |\frac{\partial d}{\partial x_j}|) + \Lambda_{i,j,k} f(\phi) \equiv L(\phi, d) + \Lambda_{i,j,k} f(\phi) \tag{1.16}$$

with $\text{sgn}(\phi) = 2H(\mathbf{x}) - 1$ denotes the signum function, $d_0(\mathbf{x}, t) = \phi(\mathbf{x}, t)$, and

$$\Lambda_{i,j,k} f(\phi) = \frac{\int_{\Omega_{i,j,k}} H'(\phi) L(\phi, d) d\Omega_{i,j,k}}{\int_{\Omega_{i,j,k}} H'(\phi) f(\phi) d\Omega_{i,j,k}}; \quad f(\phi) = H'(\phi)/\nabla|\phi| \tag{1.17}$$

The last term in the above expression is added to keep the bubble volume constant during the reinitialisation procedure. The equation is iterated until $|\nabla d| = 1$. The corrected ϕ–field is then obtained by setting $\phi(x, t) = d(x, \varepsilon)$, where ε is the time elapsed for Eq. (1.16) to reach convergence. In TransAT, Eq. (1.16) is solved after each advection step of the Level Set equation using the non-oscillatory (WENO) 3rd order scheme.

1.3.3   Fast-marching re-distancing

This is an extreme case of the narrow band method, in that the band in question is taken as a single cell. Of interest in Level Set methods is to preserve the normal distribution of the iso-contours of function $\phi(x)$ through the Eikonal equation:

$$|\nabla \phi| = f(x); \quad x \in R^n \tag{1.18}$$

with boundary conditions $\phi(x) = g(x), x \in \Gamma \subset R^n$. In the simplest case where the speed function $f(x)$ is a constant, usually equal to one, then the solution of the Eikonal equation above will represent the shortest distance from a point x to the zero distance curve, usually given by Γ, that is if $g(x) = 0$. To construct an approximation to the Eikonal equation for a grid point x using the surrounding points x_i, x_n, first define the unit directional vector pointing from point x_i to point x as $P_i = (x - x_i)/||x - x_i||$. Then let $v_i(x)$ be the value of the approximate directional derivative in direction P_i and point x.

We then solve a quadratic equation for the distance $\phi(x)$ in the form

$$(a^T Q a)\phi(x)^2 + (2a^T Q b)\phi(x) + (b^T Q b) = f(x)^2 = 1 \tag{1.19}$$

where Q is defined as $Q = (PP^T)^{-1}$ and the vectors a and b by their respective constituents a_i and b_i. This equation is then solved to find two roots of which the largest one is taken as a possible new distance for $\phi(x)$. This new distance can only be accepted if the update comes from within the polygon spanned by $x, x_i, c \ldots, x_n$ and if the calculated distance value is smaller than the old one. Thus we only update if $\phi(x) < \phi^{old}(x)$.

1.3.4   Thin-film boundary conditions

For flows with very low Capillary numbers, there exists a thin water film between the gas phase and the wall. A thin-film boundary condition can then be defined. The viscosity at the film–boundary wall is set so as to satisfy the shear according to Couette flow. For a liquid film condition we get (see Fig. 1.1),

---
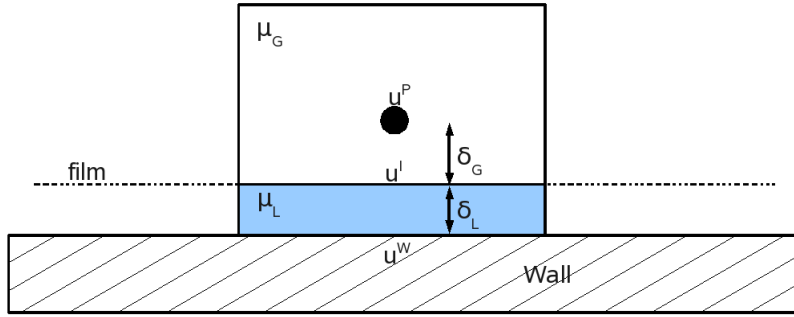
Figure 1.1: Sketch for thin-film boundary condition

$$(u_i^P - u_i^I)\frac{\mu_G}{\delta_G} = (u_i^I - u_i^W)\frac{\mu_L}{\delta_L} \tag{1.20}$$

The interface velocity (tangential to the wall) u^I is then given as,

$$u_i^I = \frac{u_i^P \frac{\mu_G}{\delta_G} + u_i^W \frac{\mu_L}{\delta_L}}{\frac{\mu_G}{\delta_G} + \frac{\mu_L}{\delta_L}} \tag{1.21}$$

The effective viscosity is then set according to the following equation,

$$(u_i^P - u_i^W)\frac{\mu_{eff}}{(\delta_G + \delta_L)} = (u_i^I - u_i^W)\frac{\mu_L}{\delta_L} \tag{1.22}$$

Or simplifying Eq. (1.22) we obtain,

$$\mu_{eff} = \frac{\mu_L \mu_G (\delta_G + \delta_L)}{(\mu_L \delta_G + \mu_G \delta_L)} \tag{1.23}$$

1.3.5   Marangoni effect

Marangoni force can be modelled, which will make the surface tension coefficient depend on temperature

$$\sigma(T) = \sigma_0 \frac{(T_{crit} - T)}{(T_{crit} - T_0)} \tag{1.24}$$

where, σ_0 is the surface tension coefficient at temperature T_0, and T_{crit} is the temperature of the material at which surface tension is zero.

The thermo-capillary (Marangoni) contribution to the Navier-Stokes equation is the projection tangential to the interface of the shear stress generated by the temperature dependence of the surface tension and writes:

$$F_m = \nabla.(\frac{\partial \sigma}{\partial T}\nabla T) \tag{1.25}$$

1.3.6   Dynamic contact angle treatment

The treatment of wetting dynamics is based on the physical forces associated with triple lines (Friess & Lakehal, 2004; Narayanan & Lakehal, 2006). An additional triple-line contact force (c_i) is included in the momentum equation; this extended momentum equation provides a physically adequate description of wetting dynamics, eliminating the need for any particular boundary condition specifying the contact angle. The triple-line force (c_i) is based on a consideration of interfacial free energy. Accordingly, it contains only two parameters: the interfacial tension between the fluids γ and the equilibrium contact angle θ_{eq}.

$$c_i = \gamma(\cos(\theta_{eq}) - \cos(\theta_{dy}))\delta^t b_i \tag{1.26}$$

where θ_{dy} is the instantaneous dynamic contact angle, δ^t is a smooth Dirac delta function vanishing everywhere except near the triple lines, with the property that for any volume V, the integral $\int_V \delta^t dV$ is equal to the length of the triple line segment contained in V, and b is the unit vector normal to the triple line and parallel to the wall surface. The triple-line force, is obtained by considerations similar to the derivation of Youngs Law and is referred to as the unbalanced Young force (De Gennes, 1985).

In addition, the shear stress is assumed to have a logarithmic profile as it nears the contact line (Qian *et al.*, 2004). At distances less than a slip length from the triple line, full slip is assumed. In the finite volume containing the triple line, the integrated shear stress is applied. The slip length is taken to be a small value $\approx 10^{-9}$. This formulation resolves the stress singularity that arises due to the no–slip boundary condition.

1.4   Phase change modelling

In the presence of phase change, equation (1.11) is rewritten

$$\frac{\partial \phi}{\partial t} + u_j \frac{\partial \phi}{\partial x_j} = -\frac{\rho \, \dot{m}''}{\rho_l \, \rho_g} \left| \frac{\partial \phi}{\partial x_j} \right| \tag{1.27}$$

where $\dot{m}''$ stands for the mass transfer per unit area per unit time. A new source term also appear in the velocity divergence equation (1.2), which becomes

$$\frac{\partial u_j}{\partial x_j} = \dot{m}'' \left(\frac{1}{\rho_g} - \frac{1}{\rho_l} \right) \delta(\phi) \left| \frac{\partial \phi}{\partial x_j} \right| \tag{1.28}$$

Finally, a new source term is added to the energy equation (1.4)

$$\rho \, C_p \frac{\partial T}{\partial t} + \rho \, C_p \, u_j \frac{\partial T}{\partial x_j} = \frac{\partial}{\partial x_j} \left(\lambda \frac{\partial T}{\partial x_j} \right) + \dot{Q}''' - \dot{m}'' \delta(\phi) \Delta h_{lv} \tag{1.29}$$

It now remains to model the mass transfer term $\dot{m}''$.

1.4.1   Direct phase change

When using direct phase change, mass transfer is given by the formula

$$\dot{m} = \frac{\mathbf{q} \cdot \mathbf{n}}{\mathcal{L}} \tag{1.30}$$

$$\mathbf{q} \cdot \mathbf{n} = 2\ \lambda\ (T - T_{sat})\ \delta(\phi) \tag{1.31}$$

with $\mathcal{L}$ the latent heat.

1.4.2   Correction of saturation temperature

The saturation temperature can be locally adjusted to take into account the effect of curvature, using the equation

$$T_{sat}(\mathbf{x}) = T_{sat} \left(1 + \frac{F(\rho)\kappa(\mathbf{x})\sigma(\mathbf{x})}{2L} \right) \tag{1.32}$$

where, $F(\rho) = \rho_G^{-1} + \rho_L^{-1}$, κ is the local curvature, σ is the local surface tension coefficient, and L is the latent heat of phase change.

1.4.3   Correlation-based models

Different models are based on global correlation. In this case, local $\dot{m}$ do not vary in space and time, but the global value will change because of the changes of interfacial area. They are all based on the same expression

$$\dot{m} = h\frac{T_{sc} - T_{sat}}{\mathcal{L}} = \frac{Nu_L \lambda_L}{L_{L,\dot{m}}} \frac{T_{sc} - T_{sat}}{\mathcal{L}} \tag{1.33}$$

where Nu_L is the liquid Nusselt number, $\mathcal{L}$ is the latent heat and T_{sat} is the saturation temperature. T_{sc} and $L_{L,\dot{m}}$ are given parameters. Nu_L can be given by different correlations.

- In the Hiemenz correlation (Davis & Yadigaroglu, 2004), it is written

$$Nu_L = \frac{2}{\sqrt{\pi}} \left(\frac{\rho_L}{\rho_G} \frac{\mu_G}{\mu_L} \right)^{1/20} \sqrt{Pr_L Re_L} \tag{1.34}$$

  where

$$Re_L = \frac{\rho_L L_{L,\dot{m}} u_{L,\dot{m}}}{\mu_L} \tag{1.35}$$

  is the liquid Reynolds number, and $u_{L,\dot{m}}$ is a correlation velocity.

- Other correlations have also been proposed by Lim et al. (Lim *et al.*, 1984):

$$Nu_L = 0.534 \, Re_G^{0.58} \, Re_L^{0.09} \, Pr_L^{0.3} \tag{1.36}$$

for smooth interface, and

$$Nu_L = 0.0291 \, Re_G^{0.58} \, Re_L^{0.42} \, Pr_L^{0.3} \tag{1.37}$$

for wavy interface. In these expressions,

$$Re_G = \frac{\rho_G L_{G,\dot{m}} u_{G,\dot{m}}}{\mu_G} \tag{1.38}$$

is the liquid Reynolds number.

1.4.4   Interface Mass Transfer (IMT)

This section describes the interfacial mass transfer models that have been implemented in TransAT (Lakehal & Labois, 2011*a*). For the sake of simplicity, all of them will be written in the form

$$\frac{\dot{m}}{u'} = \frac{h}{\rho C_p u'} = f(Pr/Sc, Re_t) \tag{1.39}$$

where $\dot{m}$ is the mass transfer rate, h is the heat transfer coefficient, u' is a characteristic velocity of the flow, Pr is the Prandtl number, Sc is the Schmidt number and Re_t a turbulent Reynolds number.

- The surface-divergence model (Banerjee *et al.*, 2004; Lakehal *et al.*, 2008*b*) can be written:

$$\frac{\dot{m}}{u'} = C Sc^{-1/2} \left(0.3 \left(2.83 Re_t^{3/4} - 2.14 Re_t^{2/3} \right) \right)^{1/4} Re_t^{-1/2} \tag{1.40}$$

where $C = 0.35$ if Sc (or Pr) < 4, 0.45 otherwise. This model is adapted for low Reynolds number. It is also implemented with modifications, for the small eddy context

$$\frac{\dot{m}}{u'} = C Sc^{-1/2} \left(0.3 \left(2.83 Re_t^{3/4} - 2.14 Re_t^{2/3} \right) \right)^{1/4} Re_t^{-1/4} \tag{1.41}$$

This model is adapted for very high turbulent Reynolds numbers. Finally, an adaptive surface divergence version has been implemented

$$\frac{\dot{m}}{u'} = C Sc^{-1/2} \left(0.3 \left(2.83 Re_t^{3/4} - 2.14 Re_t^{2/3} \right) \right)^{1/4} Re_t^{-n} \tag{1.42}$$

with

$$n = \begin{cases} 0.5 & if \quad Re_{t,int} < 3000 \\ -1.89.10^{-5} Re_{t,int} + 0.56 & if \quad 3000 < Re_{t,int} < 16000 \\ 0.25 & if \quad Re_{t,int} > 16000 \end{cases} \tag{1.43}$$

where $Re_{t,int}$ is the turbulent Reynolds number at the interface. This model is adapted for high Reynolds numbers.

- The small-eddy model (Banerjee *et al.*, 1968; Theophanous *et al.*, 1976) can be written

$$\frac{\dot{m}}{u'} = 0.25 Sc^{-1/2} Re_t^{-1/4} \tag{1.44}$$

- The surface renewal model (Lakehal *et al.*, 2008a) links the mass transfer with the interfacial frictional Reynolds number $Re_\star$. It reads

$$\frac{\dot{m}}{u'} = C Sc^{-1/2} Re_\star^{-1/2} \tag{1.45}$$

where the following expression is used for C

$$C = 1.45 \, 10^{-6} Pr^2 + 6.6 \, 10^{-5} Pr + 0.0789 \tag{1.46}$$

- The Hughes-Duffey model (Hughes & Duffey, 1991) reads

$$\frac{\dot{m}}{u'} = \frac{2}{\sqrt{\pi}} Sc^{-1/2} \tag{1.47}$$

- The last model from (Coste, 2004) is inspired by the renewal model and reads

$$\frac{\dot{m}}{u'} = Sc^{-1/2} Re_t^{-1/8} \tag{1.48}$$

A turbulent Reynolds number is needed for the interfacial mass transfer model. Several choices are available in TransAT:

- The usual Reynolds number can be written $Re_t = \frac{k^2}{\nu\varepsilon}$. It is taken in the gas core flow. A length scale must be associated to this Reynolds number, it is computed as the weighted-average (in the gas side) of $\frac{k^2}{u_\infty}\varepsilon$, with the characteristic velocity being $u_\infty = min(|u|, C_\mu^{1/4}k^{1/2})$

- As an alternative to Re_t, another Reynolds number based on turbulence is available, $R_y = \frac{\sqrt{k}|\phi|}{\nu_L}$. It is also evaluated in the gas core flow.

- The shear Reynolds number reads $Re_\star = \frac{u_\star|\phi|}{\nu_L}$ with $u_\star = \sqrt{\frac{\tau}{\rho}}$ the shear velocity at the interface, ϕ the distance of the point to the interface. $u_\star$ and ϕ are taken in the gas near the interface, where $u_\star$ is at its maximum. $u_\star$ is also taken as the associated characteristic velocity.

Because they need the variables k and ε to be evaluated, Re_T and R_y can be used only when the $k - \varepsilon$ turbulence model is enabled. Otherwise, $Re_\star$ together with the surface renewal model will be used. The following table gives the available interfacial mass transfer models available for the different Reynolds numbers.

turbulence model	Non-dimensional number	available IMT model
$k - \varepsilon$	"Re_T"	"surfacedivg","SD_small_eddy","SD_adaptive", "Hughes-Duffey","Coste","small_eddy"
$k - \varepsilon$	"R_y"	"surfacedivg", "Hughes-Duffey","Coste","small_eddy",
$k - \varepsilon$, LES, laminar flow	"$Re_\star$"	"surface_renewal"

Table 1.1: Interfacial mass transfer models available in TransAT.

Chapter 2

Phase-Average Multi-phase Flow Modelling

2.1 Ensemble-averaged Two-phase Flow Models

We consider a mixture of two incompressible phases. Thus, the following equations are solved (Drew & Passman, 1998):

$$\frac{\partial \rho^m}{\partial t} + \frac{\partial}{\partial x_j}\left(\rho^m V_j^m\right) \quad = \quad 0$$

$$\rho_G \frac{\partial \alpha_G}{\partial t} + \rho_G \frac{\partial}{\partial x_j}\left(\alpha_G V_{G_j}\right) \quad = \quad S_{\alpha_G} \tag{2.1}$$

$$\frac{\partial \rho^m V_i^m}{\partial t} + \frac{\partial}{\partial x_j}\left(\rho^m V_i^m V_j^m\right) \quad = \quad -\frac{\partial p^m}{\partial x_i} + \frac{\partial}{\partial x_j}\left(2(\mu^m + \mu_T)S_{ij}^m\right) + S_{\text{mom}}^{\text{drift}}$$

$$\rho^m C_p^m \frac{\partial T^m}{\partial t} + \rho^m C_p^m V_j^m \frac{\partial T^m}{\partial x_j} = \frac{\partial}{\partial x_j}\left(\lambda^m \frac{\partial T^m}{\partial x_j}\right) + \dot{Q}''' \tag{2.2}$$

where the subscript G denotes the gas phase, m denotes a mixture property, and T stands for mixture turbulent property. In the following, the subscript L will also be introduced for the liquid phase. α_G is the gas volume fraction and $\rho^m = \alpha_G \rho_G + \alpha_L \rho_L$ is the density of the mixture. V^m is the velocity of the mixture, p^m the mixture pressure, and T^m is the mixture temperature. S_{α_G} and $S_{\text{mom}}^{\text{drift}}$ stand for the source terms due to mass transfer and drift velocities in the mass and momentum equations, respectively.

The phasic ensemble averaged velocities split into mixture and drift velocities as follows,

$$V_{k_i} = V_i^m + V_{k_i}^d \tag{2.3}$$

The mixture velocity is defined as follows:

$$\mathbf{V}^m = \frac{\alpha_G \rho_G \mathbf{V}_G + \alpha_L \rho_L \mathbf{V}_L}{\rho^m} \tag{2.4}$$

From Eq. (2.4) it follows that,

$$\Sigma_k \, \rho_k \alpha_k V^d_{k_i} = 0 \tag{2.5}$$

and the phasic drift velocities are related to each other by,

$$V^d_{L_i} = - \left(\frac{Y_G}{Y_L} \right) V^d_{G_i} \tag{2.6}$$

where $Y_k = \alpha_k \rho_k / \rho^m$ is the mass fraction of the phase k. The slip velocity defined as $V_{s_i} = V_{G_i} - V_{L_i}$ can be further related to the gas drift velocity as,

$$V_{s_i} = V^d_{G_i} - V^d_{L_i} = \frac{V^d_{G_i}}{Y_L} \tag{2.7}$$

2.1.1 Homogeneous Model

In the homogeneous model, it is considered that both phases have the same velocity ($\mathbf{V}^d_k = 0$). The equations can then be simplified to,

$$\frac{\partial \alpha_G}{\partial t} + \frac{\partial}{\partial x_j} \left(\alpha_G V^m_j \right) \quad = \quad S_{\alpha_G}$$

$$\frac{\partial \rho^m V^m_i}{\partial t} + \frac{\partial}{\partial x_j} \left(\rho^m V^m_i V^m_j \right) \quad = \quad -\frac{\partial p^m}{\partial x_i} + \frac{\partial}{\partial x_j} \left(2(\mu^m + \mu_T) S^m_{ij} \right) \tag{2.8}$$

Only the mixture equations are solved. The divergence of the mixture velocity is zero.

$$\frac{\partial V^m_j}{\partial x_j} = 0 \tag{2.9}$$

2.1.2 Algebraic Slip Model

In this case, an algebraic model is used to estimate the relative velocity between the two phases or between the mixture and the gas phase. Thus, several drift velocity models have been implemented. With this notation, the algebraic slip model (ASM) can be written as follows,

$$\frac{\partial \rho^m}{\partial t} + \frac{\partial}{\partial x_j} \left(\rho^m V^m_j \right) = 0 \tag{2.10}$$

$$\rho_G \frac{\partial \alpha_G}{\partial t} + \rho_G \frac{\partial}{\partial x_j} \left(\alpha_G (V_j^m + V_{G_j}^d) \right) = 0 \tag{2.11}$$

$$\frac{\partial \rho^m V_i^m}{\partial t} \quad + \quad \frac{\partial}{\partial x_j} \left(\rho^m V_i^m V_j^m + \rho^m \frac{Y_G}{Y_L} V_{G_i}^d V_{G_j}^d \right) = -\frac{\partial p^m}{\partial x_i} + \frac{\partial}{\partial x_j} (2(\mu^m + \mu_T) S_{ij}^m) \tag{2.12}$$

The divergence of the mixture velocity is given by,

$$\frac{\partial V_j^m}{\partial x_j} = \frac{\rho_G - \rho_L}{\rho_L} \frac{\partial}{\partial x_j} (\alpha_G V_{G_j}^d) \tag{2.13}$$

Models for gas drift velocity V_G^d must now be derived.

2.1.3   Algebraic slip model with drag forces

Ishii & Mishima (1984) have written the drag-induced momentum transfer term as

$$M_G = -\frac{3}{8} C_D \frac{\alpha_G \rho_L}{R_b} \left| V_G^d \right| V_G^d \tag{2.14}$$

where C_D is the drag coefficient and R_b the bubble radius.

Then, Manninen & Taivassalo (1996) derived from the conservation equations the following expression, neglecting diffusion terms due to turbulent fluctuations and assuming the local equilibrium.

$$M_G = \alpha_G \frac{\rho_m - \rho_G}{\rho_m} \nabla p \tag{2.15}$$

From these equations, an expression for the gas drift velocity can be found, assuming that all bubbles have the same radius R_b.

$$V_{G_i}^d = -\frac{16}{3} \frac{Y_L R_b^2}{C_d Re_b \mu_L} \frac{\rho_m - \rho_G}{\rho_m} \frac{\partial p^m}{\partial x_i} \tag{2.16}$$

where $Re_b = \dfrac{\rho_L \left| V_G^d \right| 2R_b}{\mu_L}$ is the bubble Reynolds number. Introducing the friction factor $\mathcal{F}$, the drag coefficient can be written

$$C_D = \frac{24}{Re_b} \mathcal{F} \tag{2.17}$$

and the drift velocity is rewritten

$$V_{G_i}^d = -\frac{2}{9} \frac{Y_L R_b^2}{\mathcal{F} \mu_L} \frac{\rho_m - \rho_G}{\rho_m} \frac{\partial p^m}{\partial x_i} \tag{2.18}$$

Friction factor remains to be modelled. In the Stokes Regime, it is simply

$$\mathcal{F} = 1 \tag{2.19}$$

This model is adapted for very small bubbles Reynolds number, usually less than 2.

Schiller & Naumann (1933) proposed the friction factor coefficient as:

$$\mathcal{F} = 1 + 0.15 Re_b^{0.687}. \tag{2.20}$$

Clift (cited in Crowe *et al.* (1998)) developed a model that is adapted to bubble Reynolds numbers up to 1000. In this model, friction factor is written

$$\mathcal{F} = 1 + 0.15 Re_b^{2/3} + 0.015 \left(\frac{Re_b}{1 + \dfrac{4.25\,10^4}{Re_b^{1.16}}} \right) \tag{2.21}$$

The model derived by Tomiyama (1998a) also takes into account the shape of the bubbles, using the Eötvös number $Eo = \dfrac{|\rho_L - \rho_g|\,||g||\,(2R_b)^2}{\sigma}$, where $||g||$ is the gravitational acceleration and σ the surface tension. The friction factor is then given (for highly contaminated system here):

$$\mathcal{F} = \text{Max} \left(1 + 0.15 Re_b^{0.687}, \frac{1}{9}\frac{Eo}{Eo + 4} Re_b \right) \tag{2.22}$$

2.1.4   Algebraic slip model with drag and lift forces

The expression of the lift force is given by Drew & Passman (1998)

$$F_L = -C_L \alpha_G \rho_L \left(V_L - V_g \right) \wedge \left(\nabla \wedge u_L \right) \tag{2.23}$$

Momentum transfer term 2.14 can then be rewritten as

$$M_G = -\frac{3}{8} C_D \frac{\alpha_G \rho_L}{R_b} \left| V_G^d \right| V_G^d - C_L \frac{\alpha_G \rho_L}{Y_L} V_G^d \wedge \left(\nabla \wedge u_L \right) \tag{2.24}$$

and solving this equation will give the gas drift velocity. In this expression, lift coefficient is still unknown. It can be taken as a constant, with values of $\frac{1}{4}$ (Drew & Passman, 1998) or $\frac{1}{2}$ (Drew & Lahey, 1987) proposed in the literature for bubbly flows. Tomiyama (1998b) derived a more complex model, in accordance with deformable bubbles correlation. It evaluates the long axis d_H of a deformable bubble, and proposes to compute the lift coefficient based on this axis. The model can then be written

$$Eo = \frac{|\rho_L - \rho_g| \, ||g|| \, (2R_b)^2}{\sigma} \tag{2.25}$$

$$d_H = 2Re_b \left(1 + 0.163 Eo^{0.757}\right)^{1/3} \tag{2.26}$$

$$Eo_d = \frac{|\rho_L - \rho_g| \, ||g|| d_H^2}{\sigma} \tag{2.27}$$

$$C_L = \begin{cases} \text{Min} \left(0.288 \text{tanh} \left(0.121 \, Re_b\right), \right. \\ \left. \quad 0.00105 \, Eo_d^3 - 0.0159 \, Eo_d^2 - 0.0204 \, Eo_d + 0.474\right) & Eo_d < 4 \\ 0.00105 \, Eo_d^3 - 0.0159 \, Eo_d^2 - 0.0204 \, Eo_d + 0.474 & 4 \leq Eo_d < 10 \\ -0.27 & Eo_d \geq 10 \end{cases} \tag{2.28}$$

2.1.5   Wall lubrication force

When the lift force is used an unrealistic accumulation of small bubbles at the wall could appear. To counterbalance this effect an additional wall lubrication force is typically included. The expression of the wall lubrication force is given by Rzehak *et al.* (2012):

$$F_{WL} = C_{WL} \frac{\alpha_G}{Y_L} \rho_L |V_G^d|^2 n_W \left[1 - \exp\left(\frac{y_w}{R_b}\right)\right], \tag{2.29}$$

where n_W is the unit vector perpendicular to the wall, pointing into the fluid. The second part of the force was added to keep in account the fact that the lubrication force acts only close to the wall in a exponentially way and not at the center of the vessel. Momentum transfer term 2.14 can then be rewritten as:

$$M_G = -\frac{3}{8} C_D \frac{\alpha_G \rho_L}{R_b} \left|V_G^d\right| V_G^d - C_L \frac{\alpha_G \rho_L}{Y_L} V_G^d \wedge (\nabla \wedge u_L)$$
$$+ C_{WL} \frac{\alpha_G \rho_L}{Y_L} |V_G^d|^2 n_W \left[1 - \exp\left(\frac{y_w}{R_b}\right)\right]. \tag{2.30}$$

In TransAT, different models are available. According to Antal *et al.* (1991), the expression of the C_{WL} coefficient was derived based on calculation of the flow field around a two dimensional circular bubble in potential flow as:

$$C_{WL} = \max \left\{0, \frac{-0.01}{2R_b} + \frac{0.05}{y_W}\right\}. \tag{2.31}$$

Based on the observation of single bubble trajectories, Tomiyama *et al.* (1995) proposed this formulation:

$$C_{WL} = C_W \left(\frac{R_b}{y_W^2}\right). \tag{2.32}$$

with the coefficient C_W that depends on the Eotvos number. According to the Tomiyama formulation, the coefficient C_W of the Eq. 2.32 is:

$$C_W = \begin{cases} 0.47 & Eo < 1 \\ e^{-0.933Eo+0.179} & 1 < Eo \leq 5 \\ 0.00599Eo - 0.0187 & 5 < Eo \leq 33 \\ 0.179 & 33 < Eo \end{cases}. \tag{2.33}$$

Another correlation of the C_W, depending on the Eotvos number, was proposed by Hosokawa *et al.* (2002) as:

$$C_{WL} = 0.0217Eo. \tag{2.34}$$

Frank *et al.* (2004) generalized the Tomiyama model to produce the Frank Wall Lubrication force model, that is given by:

$$C_{WL} = C_W \cdot \max \left\{ 0, \frac{1}{6.8} \cdot \frac{1 - \frac{y_W}{20R_b}}{y_W \cdot \left(\frac{y_W}{20R_b} \right)^{0.7}} \right\}, \tag{2.35}$$

where C_W is the coefficient defined in 2.33, that preserves the same dependence on Eotvos number as the Tomiyama model.

2.1.6   Turbulent dispersion

The drift velocity models of the previous sections do not take into account the effect of the turbulence. In this aim, Ishii (1975) proposed a term to be added to the gas drift velocity:

$$V_{g_i}^d = V_{g,\text{no diffusion}_i} + \alpha_L \frac{\nu_T}{Pr_T} \frac{\partial \alpha_G}{\partial x_i} \tag{2.36}$$

where ν_T is the turbulent kinematic viscosity and Pr_T is the turbulent Schmidt number.

2.2   Phase change modelling

Phase change phenomenon is divided into phase change happening in the bulk and phase change happening near a wall (heated or cooled). The latter is called heterogeneous phase change.

2.2.1   Phase change in the bulk

Phase change happening in the bulk of the fluid (away from the flow boundaries) can be phenomenologically split into different phase change modes, such as,

- Dispersed phase change

- Interfacial phase change

- Cavitation

- Homogeneous condensation

where the first two are thermally limited phase change phenomena and the last two are inertial phase change phenomena where the spontaneous phase change is related to rapid pressure changes. Currently, homogeneous condensation models are not available in TransAT.

Dispersed-phase phase change

This mode of phase change is defined as phase change that happens under thermal non-equilibrium under conditions where the phases are well mixed. The phase change rate is limited by the temperature difference ($T - T_{sat}$ and the interfacial area density. The model available in TransAT is based on the Ranz-Marshall Nusselt number model (Ranz & Marshall, 1952). The mass transfer rate (kg/m^3) is given as,

$$\dot{m}''' = \frac{q'' \, a}{L}; \qquad a = \frac{6\alpha_d}{d_p} \tag{2.37}$$

$$q'' = \mathrm{Nu}\frac{\lambda}{d_p}(T - T_{\mathrm{sat}}); \qquad \mathrm{Nu} = 2 + \mathrm{Re}^{\frac{1}{2}}\mathrm{Pr}^{\frac{2}{3}} \tag{2.38}$$

where $\dot{m}'''$ is the volumetric phase change rate in $kg/(m^3 s)$, q'' is the interfacial heat flux, a is the interfacial area density, L is the latent heat of vaporization or condensation, Nu is Nusselt number, d_p is the droplet/bubble diameter, Re is the droplet Reynolds number based on the slip velocity and T_{sat} is the saturation temperature at the local pressure. The bubble/droplet diameter is specified as an input. The system can be forced into phase/thermal equilibrium by specifying ever lower values for d_p.

Interfacial phase change

The main difference between the interfacial and the dispersed phase change models is the fact that for conditions where the phases are separated, one can obtain an estimate for the real interfacial area using the gradient of the volume fraction. Interfacial phase change has been split into two cases in TransAT,

1. Interfacial thermal diffusion phase change model, and

2. Interfacial shear phase change model.

The interfacial shear phase change model is based on the proposal by Banerjee (Lakehal & Labois, 2011b) where,

$$\dot{m}''' = \frac{q'' a}{L}; \qquad a = \nabla \alpha \tag{2.39}$$

$$q'' = \text{Nu} \frac{\lambda}{\delta_{bl}} (T - T_{\text{sat}}); \qquad \text{Nu} = C\text{Re}_\tau \text{Pr}^{\frac{1}{2}} \tag{2.40}$$

$$\text{Re}_\tau = \frac{\rho u_\tau^I \delta_{bl}}{\mu} \tag{2.41}$$

where $\dot{m}'''$ is the volumetric phase change rate in $kg/(m^3 s)$, q'' is the interfacial heat flux, a is the interfacial area density, L is the latent heat of vaporization or condensation, Nu is Nusselt number, Re_τ is the interfacial shear Reynolds number based on the interfacial shear velocity u_τ^I, and T_{sat} is the saturation temperature at the local pressure.

Substitution the expression for Nu into the heat flux equation we obtain,

$$q'' = C\text{Pr}^{-\frac{1}{2}} u_\tau^I \rho C_p (T - T_{\text{sat}}); \tag{2.42}$$

where C is the only model parameter. Note that this closed form expression is a special case due the fact that the exponent of the Reynolds number in the Nusselt number expression is 1.

In case the velocities are zero, the interfacial shear phase change model will predict zero mass transfer rate. The phase change in this case can occur due to thermal non-equilibrium which propagates by diffusion. Two models are available for interfacial diffusion phase change, viz. the Schrage model and the relaxation model.

For the Schrage model the heat transfer rate is given as,

$$q'' = \frac{2A_c}{2 - A_c} \sqrt{\frac{M_w}{2\pi R}} \frac{L^2}{T_{sat}^{3/2}} \left[\frac{1}{\rho_v} - \frac{1}{\rho_l} \right] (T - T_{sat}) \tag{2.43}$$

where, A_c is the accommodation coefficient that is a material constant.

For the relaxation model (which is only valid for very diffusive problems) the heat transfer rate is given as,

$$q'' = (\lambda_v + \lambda_l)(T - T_{sat})\nabla \alpha \tag{2.44}$$

When the dispersed and interfacial models are both active, then the two models are blended based on the magnitude of $\nabla \alpha$, where the interfacial model is chosen if the gradient is significant and vice-versa.

Cavitation models

We start with the condition of vapour bubbles in liquid of radius R_B with a nucleate density per unit volume of liquid (n_0). If we consider a volume $\Omega = \Omega_V + \Omega_L$, then,

$$\Omega_V = \alpha_V \Omega = n_0 \Omega_L \frac{4\pi}{3} R_B^3$$

$$\alpha_V = n_0 \alpha_L \frac{4\pi}{3} R_B^3 \quad \text{or} \tag{2.45}$$

$$\alpha_V = \frac{\Omega_V}{\Omega_L + \Omega_V} = \frac{n_0 \left(\frac{4\pi}{3} R_B^3\right)}{1 + n_0 \left(\frac{4\pi}{3} R_B^3\right)} \tag{2.46}$$

where Eq. (2.46) is given in Yuan *et al.* (2001)(Eq. 5) and Eq. (2.45) is the same as given in Deimel *et al.* (2014)(Eq. 13).

The bubble radius can be expressed using Eq. (2.45) as,

$$R_B = \left(\frac{\alpha_V}{\alpha_L} \frac{3}{4\pi n_0}\right)^{1/3} \tag{2.47}$$

The other starting point for cavitation models is the simplified form of the Rayleigh-Plesset equation for bubble growth given as,

$$\frac{dR_B}{dt} = \text{sgn}(p_V - p)\sqrt{\frac{2}{3}\frac{|p_V - p|}{\rho_L}} \tag{2.48}$$

The radius grows if $p < p_V$ and shrinks if $p > p_V$. An expression for $d\alpha_V/dt$ using Eq. (2.45) is obtained by assuming that n_0 does not change with time,

$$\frac{d\alpha_V}{dt} = \alpha_V \alpha_L \frac{3}{R_B}\left(\frac{dR_B}{dt}\right) \tag{2.49}$$

The definition of mixture density ($\rho = \rho_L + \alpha_V(\rho_V - \rho_L)$) is used to simplify the mixture continuity equation to obtain,

$$\frac{\partial u_{mj}}{\partial x_j} = \frac{(\rho_L - \rho_V)}{\rho}\left(\frac{\partial \alpha_V}{\partial t} + u_{mj}\frac{\partial \alpha_V}{\partial x_J}\right) \tag{2.50}$$

under the assumption of incompressibility. Further in the absence of slip between the vapour and liquid phases (homogeneous flow), we can write the above equation as,

$$\frac{\partial u_{mj}}{\partial x_j} = \frac{(\rho_L - \rho_V)}{\rho}\left(\frac{d\alpha_V}{dt}\right) \tag{2.51}$$

Under the assumptions of incompressibility and homogeneous flow the following expression for the divergence of the velocity field is obtained,

$$\frac{\partial u_{mj}}{\partial x_j} = \left(\frac{1}{\rho_V} - \frac{1}{\rho_L}\right)\dot{m}_e''' \tag{2.52}$$

where the subscript e denotes evaporation. Using Eqs. (2.51,2.52,2.49) we obtain an expression for the evaporation rate as,

$$\dot{m}_e''' = \frac{\rho_L \rho_V}{\rho} \alpha_V \alpha_L \frac{3}{R_B} \left(\frac{dR_B}{dt} \right) \tag{2.53}$$

Sauer cavitation model

The model of Yuan *et al.* (2001) is derived by plugging Eqs. (2.48,2.47) in to Eq. (2.53) to obtain,

$$\dot{m}_e''' = \frac{\rho_L \rho_V}{\rho} \alpha_V \alpha_L \frac{3}{R_B} \operatorname{sgn}(p_V - p) \sqrt{\frac{2}{3} \frac{|p_V - p|}{\rho_L}} \tag{2.54}$$

$$R_B = \left(\frac{\alpha_V}{\alpha_L} \frac{3}{4\pi n_0} \right)^{1/3} \tag{2.55}$$

The problem with this model arises due to the fact that in a pure liquid $\alpha_V = 0$ which makes the evaporation rate zero. Therefore an initial nucleation radius is introduced (R_0) and the related α_{V0} can be calculated based on Eq. (2.46). The final model is written as,

$$\dot{m}_e''' = \frac{\rho_L \rho_V}{\rho} (\alpha_V + \alpha_{V0})(\alpha_L - \alpha_{V0}) \frac{3}{R_B} \operatorname{sgn}(p_V - p) \sqrt{\frac{2}{3} \frac{|p_V - p|}{\rho_L}} \tag{2.56}$$

$$R_B = \left(\frac{(\alpha_V + \alpha_{V0})}{(\alpha_L - \alpha_{V0})} \frac{3}{4\pi n_0} \right)^{1/3} \tag{2.57}$$

$$\alpha_{V0} = \frac{n_0 \left(\frac{4\pi}{3} R_0^3 \right)}{1 + n_0 \left(\frac{4\pi}{3} R_0^3 \right)} \tag{2.58}$$

The model has two input parameters n_0 and R_0, where typical values are $n_0 = 10^8$ and $R_0 = 10^{-6}$ as in Deimel *et al.* (2014).

Singhal cavitation model

Eq. (9) in Singhal *et al.* (2002) was found to be not correct. This means that Eq. (10) in Singhal *et al.* (2002) should actually be,

$$\frac{D\rho}{Dt} = -(\rho_l - \rho_v)(n4\pi)^{1/3}(3\alpha)^{2/3}(1 - \alpha)^{4/3} \frac{D\mathcal{R}_B}{Dt} \tag{2.59}$$

using the notation of Singhal *et al.* (2002). In fact, with this correction the basic unadulterated expression for the mass transfer rate (Singhal *et al.* (2002):Eq. (13)) is the same as Eq. (2.53)

In this model the closure for R_B is provided using critical Weber number considerations based on stable bubble size under aerodynamic drag.

$$We_{d\infty} = \frac{\rho_L(u_{jL} - u_{jV})^2 D_{d\infty}}{\sigma} \tag{2.60}$$

where $D_{d\infty}$ is the bubble diameter at the end of the fragmentation process (stable diameter). Typically a value between $5 < We_{d\infty} < 20$ is quoted in the literature (Kolev, 2002). By rearranging equation 2.60 for $D_{d\infty}$, we get

$$R_B = \frac{D_{d\infty}}{2} = \frac{We_{d\infty}\sigma}{2\rho_L v_{\text{rel}}^2} \tag{2.61}$$

Substituting Eq. (2.61) into Eq. (2.53) we obtain

$$\dot{m}_e''' = \frac{\rho_L \rho_V}{\rho} \alpha_V \alpha_L \frac{3(2\rho_L v_{\text{rel}}^2)}{We_{d\infty}\sigma} \operatorname{sgn}(p_V - p)\sqrt{\frac{2}{3}\frac{|p_V - p|}{\rho_L}} \tag{2.62}$$

In order to derive the exact model given in Singhal *et al.* (2002), we rearrange the equation as follows,

$$\dot{m}_e''' = \left[\frac{6v_{\text{rel}}^2}{We_{d\infty}\sigma}\right]\left(\frac{\rho_L}{\rho}\right)(\rho_V \alpha_V)(\rho_L \alpha_L)\operatorname{sgn}(p_V - p)\sqrt{\frac{2}{3}\frac{|p_V - p|}{\rho_L}} \tag{2.63}$$

Expressing the term in the square brackets as $C V_{\text{ch}}/\sigma$, where C is a (dimensional with units of velocity) empirical constant, and V_{ch} is a characteristic velocity, we get,

$$\dot{m}_e''' = C\frac{V_{\text{ch}}}{\sigma}\left(\frac{\rho_L}{\rho}\right)(\rho_V \alpha_V)(\rho_L \alpha_L)\operatorname{sgn}(p_V - p)\sqrt{\frac{2}{3}\frac{|p_V - p|}{\rho_L}} \tag{2.64}$$

The final form of the model is obtained by using different coefficients for the evaporation and condensation rates. In addition, the volume fraction of vapour is removed from the evaporation rate equation and the volume fraction of of liquid is removed from the condensation rate equation. This is necessary since for a pure liquid α_V is initially zero thereby making the evaporation rate zero. Introducing these changes, we get

$$\dot{m}_e''' = C_e\frac{V_{\text{ch}}}{\sigma}\left(\frac{\rho_L}{\rho}\right)\rho_V(\rho_L \alpha_L)\operatorname{sgn}(p_V - p)\sqrt{\frac{2}{3}\frac{|p_V - p|}{\rho_L}} \tag{2.65}$$

$$\dot{m}_c''' = C_c\frac{V_{\text{ch}}}{\sigma}\left(\frac{\rho_L}{\rho}\right)\rho_L(\rho_V \alpha_V)\operatorname{sgn}(p - p_V)\sqrt{\frac{2}{3}\frac{|p_V - p|}{\rho_L}} \tag{2.66}$$

$$\tag{2.67}$$

The volume fraction need to be converted to mass fraction in order to compare with Eqs. (15-16) in Singhal *et al.* (2002). We obtain,

$$\dot{m}_e''' \quad = \quad C_e \frac{V_{\text{ch}}}{\sigma} \rho_V \rho_L \left[\frac{2}{3} \frac{(p_V - p)}{\rho_L} \right]^{1/2} Y_L \tag{2.68}$$

$$\dot{m}_c''' \quad = \quad C_c \frac{V_{\text{ch}}}{\sigma} \rho_L \rho_L \left[\frac{2}{3} \frac{(p - p_V)}{\rho_L} \right]^{1/2} Y_V \tag{2.69}$$

$$\tag{2.70}$$

The model is closed by choosing $V_{\text{ch}} = \sqrt{k}$ and the velocities $C_e = 0.02$ and $C_c = 0.01$. The effect of turbulence on the vapour pressure is accounted for by writing,

$$p_{\text{turb}}' = 0.39 \rho k \tag{2.71}$$

$$p_V = p_{\text{sat}} + p_{\text{turb}}'/2 \tag{2.72}$$

Implementation in TransAT

The evaporative mass transfer rate is written using an indicator function due to the change in coefficients and the appropriate volume fraction as follows.

$$\dot{m}_e''' = \frac{V_{\text{ch}}}{\sigma} \left(\frac{\rho_L^2 \rho_V}{\rho} \right) [(1 - I_e)C_c \alpha_V + I_e C_e \alpha_L] \, \text{sgn}(p_V - p) \sqrt{\frac{2}{3} \frac{|p_V - p|}{\rho_L}} \tag{2.73}$$

where the indicator function I_e is 1 if $p < p_V$ and 0 other wise and can be expressed as

$$I_e = \frac{1 + \text{sgn}(p_V - p)}{2} \tag{2.74}$$

2.2.2 Wall Heat Flux Modeling during Subcooled Nucleate Boiling

General Formulation

For the liquid phase, the heat flux from the wall to the liquid are transferred through the following means: heat convection to the liquid phase away from the nucleation sites, microlayer evaporation and quenching. In nucleate subcooled boiling, the wall heat is utilised in forming bubbles and heating the liquid. According to Kurul & Podowski (1991), the total convective heat flux from the wall is the sum of three models:

$$q_{NB}'' = q_{1\phi}'' + q_e'' + q_Q'' \tag{2.75}$$

where $q_{1\phi}''$ is the single-phase convective heat flux, q_e'' is the heat flux associated with phase change and q_Q'' is the quenching flux, during the dwell time.

Single-Phase Heat Flux

In the portion of the wall unaffected by the bubbles, the heat transfer from the wall to the liquid can be determined by:

$$q_{1\phi}^{''} = A_{1\phi}^{''} St_P \rho_l c_{pl} u_l \left(T_w - T_l\right) \tag{2.76}$$

Now, $A_{1\phi}^{''}$ is the fraction of the wall unaffected by the nucleation sites, ρ_l is the liquid density, c_{pl} is the liquid specific heat, T_w is the wall temperature, T_l is the temperature of the liquid. St_P is the Stanton Number calculated from heat transfer correlation in terms of the local liquid velocity and Prandtl Number. St_P could be written as,

$$St_P = \frac{Nu}{Re \cdot Pr} \tag{2.77}$$

where Nu, the Nusselt Number, is provided by the Ranz-Marshall correlation.

$$Nu = 2 + 0.6 Re^{\frac{1}{2}} Pr^{0.3} \tag{2.78}$$

or from the correlation found in Vyskocil & Macek (2008)

$$Nu = max\left(\sqrt{\frac{4Pe}{\pi}}, \frac{12}{\pi}, 2\right) \tag{2.79}$$

Re, Pr and Pe are the Reynolds, Prandtl and Peclet numbers respectively.

Evaporative Heat Flux

Taking into account the effect of area overlapping between the neighboring sites, the the evaporative heat flux , $q_e^{''}$ is given by E. Krepper & Egorov (2007), becomes

$$q_e^{''} = \frac{2}{3} \frac{d_{det}}{a_b^2} \rho_v A_{2\phi}^{''} f_{det} N^{''} h_{fg} \tag{2.80}$$

where ρ_v is the vapor density, h_{fg} is the latent heat of vaporisation, a_b^2 is the bubble influence factor having a value of 2. The area fraction under the influence of bubbles, $A_{2\phi}^{''}$ is given by

$$A_{2\phi}^{''} = min\left(\pi \frac{(a_b d_{det})^2}{4}, 1\right) \tag{2.81}$$

where d_{det} is the bubble diameter at departure, which depends on the local liquid subcooling:

$$d_{det} = min\left(0.6\,[mm]\, e^{\left(-\frac{\Delta T_{sub}}{45}\right)}, 1.4\,[mm]\right) \tag{2.82}$$

Here, ΔT_{sub} is the difference between the saturation temperature and the liquid temperature.

$$\Delta T_{sub} = T_{sat} - T_l \tag{2.83}$$

In Eq. 2.80, f_{det} is the frequency of nucleation. In general, A simpler estimation of the bubble departure frequency as ratio of the terminal rise velocity over the bubble departure diameter is:

$$f_{det} = \sqrt{\frac{4g\left(\rho_l - \rho_g\right)}{3d_{det}\rho_l}} \tag{2.84}$$

where g is the acceleration due to gravity. $N^{''}$ is the nucleation site density

$$N^{''} = 185\left(T_w - T_l\right)^{1.805} \tag{2.85}$$

Quenching Heat Flux

$$q_Q^{''} = A_{2\phi}^{''}h_Q\left(T_w - T_L\right) \tag{2.86}$$

where h_Q is the quenching heat transfer, given by

$$h_Q = \frac{2}{\sqrt{\pi}}f_{det}\sqrt{t_w k_l \rho_l c_{pl}} \tag{2.87}$$

where, k_l is the liquid thermal conductivity. Here, t_w is the waiting time between the departure and the inception of the next bubble. It is assumed that the waiting time takes 80% of the bubble departure period. Hence,

$$t_w = \frac{0.8}{f_{det}} \tag{2.88}$$

To close the model, Eq. 2.75 can be solved iteratively for the local wall temperature T_w

2.3   Ensemble-averaged N-phase flow

2.3.1   N-phase model

A mixture of N phases can be simulated with the following set of equations. Definitions are given below

$$\frac{\partial}{\partial t} \rho^m + \frac{\partial}{\partial x_j} \left(\rho^m V_j^m \right) = 0 \tag{2.89}$$

$$\rho_k \frac{\partial \alpha_k}{\partial t} + \rho_k \frac{\partial}{\partial x_j} \left(\alpha_k V_{k_j} \right) = S_k \tag{2.90}$$

$$\frac{\partial}{\partial t} \left(\rho^m V_i^m \right) + \frac{\partial}{\partial x_j} \left(\rho^m V_i^m V_j^m \right) = -\frac{\partial p}{\partial x_i} + \frac{\partial}{\partial x_j} \left(2(\mu^m + \mu_T) S_{ij}^m \right) + S_{\text{mom}}^{\text{drift}} \tag{2.91}$$

$$\rho^m C_p^m \frac{\partial T^m}{\partial t} + \rho^m C_p^m u_j \frac{\partial T^m}{\partial x_j} = \frac{\partial}{\partial x_j} \left(\left(\frac{\mu^m}{Pr} + \frac{\mu_T^m}{Pr_T} \right) \frac{\partial T^m}{\partial x_j} \right) \tag{2.92}$$

$$\sum_{k=1}^{N} \alpha_k = 1 \tag{2.93}$$

with the subscript k denoting the phase index and the superscript m denoting a mixture variable, and α being the volume fraction. Mixture variables are defined as follows

$$\text{Mixture density} \qquad \rho^m = \sum_{k=1}^{N} \alpha_k \rho_k \tag{2.94}$$

$$\text{Mixture velocity} \qquad V^m = \frac{\sum_{k=1}^{N} \alpha_k \rho_k V_k}{\rho^m} \tag{2.95}$$

$$\text{Mixture heat capacity} \quad \rho^m C_p^m = \sum_{k=1}^{N} \alpha_k \rho_k C_{p,k} \tag{2.96}$$

$$\text{Mixture viscosity} \qquad \mu^m = \sum_{k=1}^{N} \alpha_k \mu_k \tag{2.97}$$

Note also that mixture viscosity can also be modelled. This will be detailed in the following section.

2.3.2   Turbulence equations

For modelling the effect of turbulence for the N-phase flow, only the turbulent kinetic energy k and dissipation rate ε of the mixture are solved for. Also, it is assumed that all the constants of the $k - \varepsilon$ model are the standard values for single phase flow. Equations for the turbulent variables can then be written

$$\frac{\partial \rho^m k}{\partial t} + \frac{\partial}{\partial x_j} \left(\rho^m u_j k \right) = \frac{\partial}{\partial x_j} \left(\frac{\mu_T}{\sigma_k} \frac{\partial k}{\partial x_j} \right) + P - \rho^m \varepsilon \tag{2.98}$$

$$\frac{\partial \rho^m \varepsilon}{\partial t} + \frac{\partial}{\partial x_j} \left(\rho^m u_j \varepsilon \right) = \frac{\partial}{\partial x_j} \left(\frac{\mu_T}{\sigma_\varepsilon} \frac{\partial \varepsilon}{\partial x_j} \right) + \frac{\varepsilon}{k} \left(c_{1,\varepsilon} P - c_{2,\varepsilon} \rho^m \varepsilon \right) \tag{2.99}$$

2.4 Mixture viscosity

2.4.1 Suspension viscosity model

In a suspension, the flow is disturbed by the presence of a dispersed phase. If the concentration of the dispersed phase increases, the particle or droplet will feel an increased resistance of the flow, which results in a higher drag coefficient. This can be taken into account by modifying the mixture viscosity (Ishii & Zuber, 1979; Hallanger *et al.*, 1995; Manninen & Taivassalo, 1996). In this section, subscript c denotes continuous phase, while d denotes dispersed phase.

2.4.2 Suspended drops or bubbles

For a mixture including suspended drops or particles, Ishii & Zuber (1979) developed an apparent viscosity expression, which reads

$$\mu_m = \mu_c \left(1 - \alpha_d\right)^{-2.5 \frac{\mu_d + 0.4\mu_c}{\mu_d + \mu_c}} \tag{2.100}$$

2.4.3 Solid suspensions

Several correlations are available for suspensions of solid particles. Ishii & Zuber (1979) propose the following expression

$$\mu_m = \mu_c \left(1 - \frac{\alpha_d}{\alpha_{CP}}\right)^{-2.5\alpha_{CP}} \tag{2.101}$$

with α_{CP} is the close packing volume fraction, usually taken between 0.62 and 0.65 for solid particles.

Mooney (cited in Manninen & Taivassalo (1996)) proposed the following correlation

$$\mu_m = \mu_c \exp\left(\frac{2.5\alpha_d}{1 - 1.4\alpha_d}\right) \tag{2.102}$$

Finally, Mills (1985) derived the following equation for a suspension of hard spheres of equal sizes

$$\mu_m = \mu_c \frac{1 - \alpha_d}{\left(1 - \frac{\alpha_d}{\alpha_{CP}}\right)^2} \tag{2.103}$$

with $\alpha_{CP} = \frac{4}{7}$.

Chapter 3

Particle Tracking Models

3.1 Mathematical formulation

3.1.1 Momentum equations

The equation governing the particle motion is the well known example given by Maxey & Riley (1983). The equation is valid for a rigid sphere in non-uniform flow such that the sphere is isolated and far from any boundary, the Reynolds number for the relative motion between the particle and the fluid is small, and the particle size is much smaller than the smallest flow length scale. The equation is given as follows,

$$
\frac{du_{p_i}}{dt} = (1 - \frac{\rho_f}{\rho_p}) g_i \quad + \quad \frac{\rho_f}{\rho_p}\frac{Du_i}{Dt} - \frac{\rho_f}{2\rho_p}\frac{d}{dt}(u_{p_i} - u_i) - \frac{18\mu}{\rho_p d_p^2}(u_{p_i} - u_i)
$$
$$
- \quad \frac{9}{\rho_p d_p}\sqrt{\frac{\mu\rho_f}{\pi}} \int_0^t \frac{d/d\tau(u_{p_i} - u_i)}{\sqrt{t - \tau}}\, d\tau \tag{3.1}
$$

where d/dt denotes the time derivative along the particle path, and D/Dt denotes the time derivative following a fluid element. The terms in the right-hand side of Eq. (3.1) are referred to as the buoyancy, fluid (due to the fluid pressure gradient and viscous stresses), added-mass, Stokes drag, and Basset forces. For the case of particles much heavier than the fluid, Elghobashi & Truesdell (1992) have shown that the only significant forces are the Stokes drag, buoyancy, and Basset forces. They also found that the Basset force was always an order of magnitude smaller than the drag and buoyancy forces.

Other forms of the forces and additional forces can be used under different circumstances.

Drag force

In the Stokes regime, drag force applied to the particle is written

$$\vec{F}_{D,Stokes} = \frac{18\mu}{\rho_p d_p^2}(\vec{u_{p_i}} - \vec{u_i})$$ (3.2)

For a higher Reynolds number based on particles, the Clift-Gauvin correlation can be used, where

$$\vec{F}_{D,CG} = f\frac{18\mu}{\rho_p d_p^2}(\vec{u_{p_i}} - \vec{u_i})$$ (3.3)

with a friction factor f being equal to

$$f = 1 + 0.15Re_p^{2/3} + 0.0175\,Re_p\left(1 + \frac{4.25\,10^{-4}}{Re_p^{1.16}}\right)^{-1}$$ (3.4)

with the particle Reynolds being defined by

$$Re_p = \frac{\rho_f|\vec{u_{p_i}} - \vec{u_i}|d_P}{\mu}$$ (3.5)

Lift force

The standard small particle (under the Stokes flow, $Re_p << 1$ condition) does not include a lift force under the assumption of uniform flow upstream of the particle. However under non-uniform fluid flow upstream of a particle a lift force exists as proposed by Saffman,

$$\vec{F}_{L,Saff} = 1.61D^2\sqrt{\frac{\mu\rho_f}{|\vec{\omega}_c|}}(\vec{u} - \vec{v}) \times \vec{\omega}_c$$ (3.6)

Auton (1987) derived the lift force acting on a sphere in shear flow under inviscid flow conditions as,

$$\vec{F}_{L,Auton} = C_L\rho_f V_p\vec{\omega}_c \times (\vec{u} - \vec{v})$$ (3.7)

For small particles, both of these lift forces are small when compared to the drag and buoyancy forces. The lift force is also small if the dispersed phase is much heavier than the fluid (solid particles or droplets in gas). However, for bubbly flow the lift force could be significant.

Magnus Lift

The lift force due to particle rotation (Magnus force) is given for low Reynolds number by Rubinow & Keller (1961) as,

$$\vec{F}_{L,Mag} = \frac{\pi}{8}d_p^3\rho_f\left[\left(\frac{1}{2}\nabla \times \vec{u} - \omega_p\right) \times (\vec{u} - \vec{v})\right]$$ (3.8)

where ω_p is the particle rotation, and $\frac{1}{2}\nabla\times\vec{u}$ is the fluid rotation at the particle position. Rewriting it in a general form with a lift coefficient $C_{L,Mag}$ we get,

$$\vec{F}_{L,Mag} = \frac{1}{2}\rho_f|\vec{u}-\vec{v}|C_{L,Mag}A\left(\frac{(\vec{u}-\vec{v})\times\omega_r}{|\omega_r|}\right) \tag{3.9}$$

where A is the projected area of the particle, and $\omega_r = \omega_p - \frac{1}{2}\nabla\times\vec{u}$ is the relative rotation between the particle and the fluid phase. The lift coefficient for low Reynolds number is then given as

$$C_{L,Mag} = \frac{d_p|\omega_p|}{|\vec{u}-\vec{v}|} \tag{3.10}$$

Lift coefficient of Oesterl & Dinh (1998)

$$C_{L,Mag} = 0.45 + (2\gamma - 0.45)\exp(-0.075\gamma^{0.4}Re_p^{0.7}) \tag{3.11}$$

where γ, which is called the *spin rate*, is given as

$$\gamma = \frac{d_p\omega_p}{2|\vec{u}-\vec{v}|} \tag{3.12}$$

where Re_p is the particle Reynolds number.

Two-way Coupling

When two-way coupling is activated the forces acting on the particles also enter the Navier-Stokes equations by means of an additional fluid-particle interaction force $\mathbf{F}^{fp}$. For example the incompressible Navier-Stokes equations become

$$\frac{\partial u_j}{\partial x_j} = 0 \tag{3.13}$$

$$\frac{\partial}{\partial t}(\rho u_i) + \frac{\partial}{\partial x_j}(\rho u_i u_j) = -\frac{\partial p}{\partial x_i} + \frac{\partial(\sigma_{ij})}{\partial x_j} + \rho\,g_i + F_i^{fp}; \quad i = 1,2,3 \tag{3.14}$$

where ρ represents the fluid density, g_i is the acceleration of gravity, μ is the molecular viscosity and σ_{ij} is the viscous stress tensor of the fluid. ρ and μ are considered as constant for these incompressible equations. Note that the Einstein summation convention applies to repeated indices.

F_i^{fp} is the component of the fluid-particle interaction force per unit volume in the cartesian direction i, $i = 1,2,3$. As reported by Narayanan *et al.* (2002), for a given grid cell m, F_i^{fp} takes the following form

$$F_{i,m}^{fp} = \sum_{n=1}^{N_p}\frac{\rho_p^n V_p^n}{\rho_f V_m}f_i^n\,W\left(\mathbf{x}^n,\mathbf{x}^m\right) \tag{3.15}$$

where n is the particle index, N_p is the total number of particles, V_p is the particle volume, ρ_f is the fluid density, V_m is the volume of the finite-volume cell, f_i is the component of the fluid-particle interaction force in direction i on a single particle located at $\mathbf{x}^n$ and W is the projection weight of the force onto the cell node m located at $\mathbf{x}^m$.

3.1.2   Particle Angular momentum equation

$$I_p \frac{d\omega_{p_i}}{dt} = T_i \tag{3.16}$$

where I_p is the moment of inertia, and T_i is the torque acting on the particle. The torque acting on a spherical particle in Stokes flow is given as

$$T_i = -\pi \mu_f d_p^3 \omega_{ri} \tag{3.17}$$

For higher Reynolds numbers (up to 1000)

$$T_i = -2.01 \mu_f d_p^3 \omega_{ri} (1 + 0.201 Re_\omega^{\frac{1}{2}}) \tag{3.18}$$

where $Re_\omega = \rho_f \omega_p d_p^2 / 4\mu_f$.

3.1.3   Temperature equation

Each particle is assumed to be represented by a uniform temperature T_p. This assumption is valid under low particle Biot (Bi_p) number conditions, where $Bi_p = Nu_p \lambda / \lambda_p$. The rate of change of particle temperature is given as:

$$\frac{dT_p}{dt} = \frac{Nu_p}{2\tau_p^T} (T_f(\mathbf{x}_p) - T_p) \tag{3.19}$$

where, Nu_p is the particle Nusselt number given as

$$Nu_p = 2 + 0.6 Re_p^{\frac{1}{2}} Pr^{\frac{1}{3}} \tag{3.20}$$

τ_p^T is the particle thermal response time defined as

$$\tau_p^T = \frac{\rho_p C_p d_p^2}{12\lambda} \tag{3.21}$$

$T_f(\mathbf{x}_p)$ is the fluid temperature at the particle position, C_p is the particle heat capacity, and λ is the fluid thermal conductivity.

3.2 Particle Dispersion

This section describes the capabilities of TransAT for particle dispersion modelling using Langevin equation. The particle dispersion model is used in combination with the Reynolds-Averaged turbulence modelling approach.

3.2.1 Langevin model

The particle fluctuation variance (σ_p) is defined as a function of the fluid fluctuation variance (σ_f) and the particle response time as:

$$\sigma_p = \sigma_f \left(1 + \frac{\tau_p}{K \tau_f} \right)^{-1/2} \tag{3.22}$$

where $\tau_f = \text{MIN}(\tau_e, \tau_r)$ is the effective eddy time scale, $\tau_p = \rho_p d_p^2 / 18\mu$ is the particle inertial response time, $K = 1 + 0.15 Re_p^{2/3}$ is the drag correction for finite Reynolds number, and $\sigma_f = \sqrt{C_\sigma k}$. The model constants C_τ and C_σ correspond to the input variables **tauL_constant** and **sigmaF_constant**, respectively and are assigned default values of 0.11 and $1.69\sqrt{C_{mu}} \approx 0.5$, respectively (Lakehal *et al.*, 1995).

In τ_f, $\tau_e = C_\tau k/\epsilon$ is the local eddy life time in an Eulerian sense, and $\tau_r = L_e/|\mathbf{u}_p - \mathbf{u}_f|$ is the time taken by the particle to travel through the eddy (residence time), where $L_e = C_\mu^{3/4} k^{3/2}/\epsilon$ is the characteristic length scale of an eddy.

The particle velocity fluctuation equation is written as follows:

$$\frac{du'_{p_i}}{dt} = -\frac{u'_{p_i}}{\tau'_{p_i}} + \sigma_p \left(\frac{2}{\tau'_{p_i}} \right)^{1/2} \zeta(t) \tag{3.23}$$

where τ'_{p_i} is the particle response time to turbulent fluctuations and $\zeta(t)$ is a random function with a Gaussian probability density distribution and zero mean. The turbulent particle response time is given as:

$$\tau'_{p_i} = \frac{\sigma_p \tau_f}{\sqrt{\sigma_p^2 + u_{ri}}} \left(1 + \frac{\tau_p}{K \tau_f} \right) \tag{3.24}$$

where u_{ri} is the terminal velocity due to action of body forces such as gravity.

3.3 Dense Particle Modelling

3.3.1 Eulerian-Lagrangian dense particle model

The Eulerian-Lagrangian formulation for dense particle flows featuring non-negligible volume fractions ($\alpha_P > 1\%$) in incompressible flow conditions is implemented in the CMFD code TransAT

as follows (mass and momentum equations for the fluid phase and Lagrangian particle equation of motion):

$$\frac{\partial \alpha \rho}{\partial t} + \frac{\partial \alpha \rho \overline{u_j}}{\partial x_j} = 0 \tag{3.25}$$

$$\frac{\partial \alpha \rho \overline{u_i}}{\partial t} + \frac{\partial \alpha \rho \overline{u_i}\,\overline{u_j}}{\partial x_j} = \frac{\partial}{\partial x_j}\left(\overline{\Pi_{ij}} - \tau_{ij}\right) + \overline{F_b} - \overline{F_P} \tag{3.26}$$

$$\frac{Du_{Pi}}{Dt} = -f_d \frac{9\mu}{2\rho_p d_P^2}\left(u_{Pi} - u_i\left[x_P(t)\right]\right) + g_i + F_{i,coll} \tag{3.27}$$

$$f_d = 1 + 0.15 Re_P^{2/3} \tag{3.28}$$

$$Re_P = \frac{\rho d_P \Delta U_{f-P}}{\mu} \tag{3.29}$$

where α is the in-cell volume of fluid ($\alpha + \alpha_P = 1$), u is the velocity of the carrier phase, u_P is the particle velocity, $u[xp]$ is the fluid velocity interpolated on to the particle position, Re_P is the particle Reynolds number, ΔU_{f-P} is the relative velocity between the particle and fluid at the particle position, Π is the sum of viscous stress σ and pressure p, τ is the turbulent stress tensor (depending whether RANS, V-LES or LES is employed to deal with turbulence). Sources terms in (3.26) denote body forces, F_b, and the rate of momentum exchange per volume between the fluid and particle phases, F_P. Various drag correlations are available in the literature to account for higher volume fractions of particles; also the fluid viscosity can be modified based on the volume fraction of particles. In (3.27), F_{coll} denotes the inter-particle stress. The momentum equation (3.26) presented here does not neglect viscous and turbulent diffusion mechanisms in the fluid phase. The inter-phase drag model in (3.27) is set according to Gydaspow (1989)

3.3.2   Four-way coupling modelling

The fluid-independent collision force F_{coll} is made dependent on the gradient of the inter-particle stress, π, using

$$F_{coll} = \frac{\nabla \pi}{\rho_p \alpha_P} \tag{3.30}$$

Collisions between particles are estimated by the isotropic part of the inter-particle stress (its off-diagonal elements are neglected.). π is modelled as a continuum stress (Harris & Crighton, 1994), viz.

$$\pi = \frac{P_S \alpha_P^{\beta(=2-5)}}{\max\left(\alpha_c - \alpha_P;\, \varepsilon\left(1 - \alpha_P\right)\right)} \tag{3.31}$$

Constant	Value	Units	TransAT
P_p	50.0	N/m^2	Ps_Snider
β	3	–	Beta_Snider
$\alpha_{p,cp}$	0.60	–	closepack
e_{pp}	1.0	–	particle_restitution

Table 3.1: Constants for Snider (2001) model.

In TransAT, the particle field is predicted in a Lagrangian way first, then high-order accurate interpolations are resorted to map the Eulerian field (to estimate π), then back again to the Lagrangian system to determine F_{coll}). The constant P_s has units of pressure, and α_c is the particle volume fraction at close packing (typically specified to be 0.6), and constant β is set according to F.M. Auzerais & Russel (1988). The ε is a small number in the order of 10^{-7}.

Collision/Contact Pressure Models

Snider Model

The collisional pressure model of Snider (2001) is defined as,

$$p_p = \frac{P_p \alpha_p^\beta}{\max[\alpha_{p,cp} - \alpha_p, \varepsilon(1 - \alpha_p)]} \tag{3.32}$$

where P_p, β are model constants and $\varepsilon = 10^{-7}$ is a small number that prevents the sign of the collision pressure from changing for $\alpha_p > \alpha_{p,cp}$. Typical values for the model constants are given in Table 3.1.

Jackson Model

The frictional collisional pressure of Johnson & Jackson (1987) is defined as,

$$p_p = \begin{cases} 0 & \text{if } \alpha_p < \alpha_{p,min} \\ F \frac{(\alpha_p - \alpha_{p,min})^r}{(\alpha_{p,cp} - \alpha_p)^s} & \text{if } \alpha_p \geq \alpha_{p,min} \end{cases} \tag{3.33}$$

where typical values for the constants are given in Table 3.2. The Jackson model is envisaged as an add-on to kinetic models for granular flows and therefore has a cut-off particle volume fraction below which it is set to zero. The Jackson model becomes qualitatively similar to the Snider model (Snider, 2001), if $\alpha_{p,min} = 0$.

In order to apply the Jackson model in Lagrangian particle tracking, the change in sign of the denominator for $\alpha_p > \alpha_{p,cp}$ must be disallowed. Therefore, the Jackson model is implemented in

Constant	Value	Units	TransAT
F	0.005	N/m^2	F_Jackson
s	5	–	S_Jackson
r	2	–	R_Jackson
$\alpha_{p,min}$	0.45	–	vfmin_Jackson
$\alpha_{p,cp}$	0.60	–	closepack

Table 3.2: Constants for Johnson & Jackson (1987) model.

TransAT in a way similar to the Snider model.

$$p_p = \begin{cases} 0 & \text{if } \alpha_p < \alpha_{p,min} \\ F\frac{(\alpha_p - \alpha_{p,min})^r}{\max[(\alpha_{p,cp} - \alpha_p)^s, \varepsilon(1 - \alpha_p)]} & \text{if } \alpha_p \geq \alpha_{p,min} \end{cases} \tag{3.34}$$

3.4   Particle-boundary collision

The modelling of particle-boundary collision in TransAT is based on the hard sphere model described in Crowe *et al.* (1998). This model is applied to interactions of particles with solid wall boundaries, embedded objects and symmetry planes.

3.4.1   Hard sphere model

The hard sphere model for particle-wall collision is based on the integrated form of the momentum equations of classical dynamics, where the deformation of the particle does not appear explicitly in the formulation.
The translational velocity $\vec{v}_p$ and angular velocity $\vec{\omega}_p$ after the collision is calculated from the corresponding quantities before collision, the coefficient of restitution e and kinetic (sliding) friction f.
The deformation of the particle upon collision is assumed to be negligible. The particles are allowed to slide along the wall, where Coulomb's friction law is applied during this process. It is assumed that once a particle has stopped sliding there is no further sliding.

The coefficient of restitution e is regarded as a property of the material and is the ratio of the normal component of impulse in the compression period to that in the recovery period:

$$e = \frac{J_n^{recov}}{J_n^{compr}} \tag{3.35}$$

Coulomb's law states that the friction force is the product of the normal force and the coefficient of kinetic friction f. The friction force results in a change of the tangential component of impulse during the sliding period according to

$$\Delta J_t = -f J_y \vec{t} \tag{3.36}$$

with $\vec{t}$ corresponding to the unit vector in the direction of tangential velocity.

Note that the particle collision model is formulated for stationary boundaries. If the boundaries are moving, the particle tangential velocities are transformed into a new, moving frame of reference, which has the same velocity as the moving boundary, before the model equations are applied. Afterwards they are transformed back to the original frame of reference.

3.4.2 Collision with wall boundary

Depending on whether the particle stops sliding during the collision process or continues throughout, the translational and angular velocity of the particle after collision are calculated as follows (assuming a plane wall with a normal vector in the positive y-direction):
If $\frac{v_y^0}{|v_p|} < -\frac{2}{7f(e+1)}$, then

$$v_x = \frac{5}{7}\left(v_x^0 - \frac{d_p}{5}\omega_z^0\right) \tag{3.37}$$

$$v_y = -e v_y^0 \tag{3.38}$$

$$v_z = \frac{5}{7}\left(v_z^0 + \frac{d_p}{5}\omega_x^0\right) \tag{3.39}$$

$$\omega_x = \frac{2 v_z}{d_p} \tag{3.40}$$

$$\omega_y = \omega_y^0 \tag{3.41}$$

$$\omega_z = -\frac{2 v_x}{d_p} \tag{3.42}$$

If $-\frac{2}{7f(e+1)} < \frac{v_y^0}{|v_p|} < 0$, then

$$v_x = v_x^0 + \varepsilon_x f(e+1)v_y^0 \tag{3.43}$$

$$v_y = -ev_y^0 \tag{3.44}$$

$$v_z = v_z^0 + \varepsilon_z f(e+1)v_y^0 \tag{3.45}$$

$$\omega_x = \omega_x^0 - \frac{5}{d_p}\varepsilon_z f(e+1)v_y^0 \tag{3.46}$$

$$\omega_y = \omega_y^0 \tag{3.47}$$

$$\omega_z = \omega_z^0 - \frac{5}{d_p}\varepsilon_x f(e+1)v_y^0 \tag{3.48}$$

The superscript 0 denotes the initial state before collision and $\varepsilon_{x,z}$ corresponds to the components of the tangential velocity unit vector in the respective direction, i.e. they satisfy the following equation.

$$\varepsilon_x^2 + \varepsilon_z^2 = 1 \tag{3.49}$$

3.4.3   Collision with symmetry boundary

When particles collide with a symmetry boundary the collision model coefficients of restitution and friction take the following values

$$e = 1.0$$
$$f = 0.0 \tag{3.50}$$

In this case the denominator of the condition for distinction becomes zero and the following relation holds for all non-zero particle velocities.

$$-\frac{2}{7f(e+1)} < \frac{v_y^0}{|v_p|} \tag{3.51}$$

The corresponding equations for the translational and rotational velocities after collision simplify to

$$v_x = v_x^0 \tag{3.52}$$

$$v_y = -v_y^0 \tag{3.53}$$

$$v_z = v_z^0 \tag{3.54}$$

$$\omega_x = \omega_x^0 \tag{3.55}$$

$$\omega_y = \omega_y^0 \tag{3.56}$$

$$\omega_z = \omega_z^0 \tag{3.57}$$

i.e. only the sign of the wall normal velocity component is changed, the remaining translational velocity components and the rotational velocities do not change, thus the total translational and rotational momentum is conserved.

Chapter 4

Hydrates Modelling

Hydrates modelling is available in TransAT in conjunction with the N-phase mixture model (See Chapter Phase-Average Mixture Models).

4.1 Hydrate Formation Kinetics

Two models have been implemented for hydrate formation: finite–rate kinetics model (Vysniauskas & Bishnoi, 1983) and instantaneous formation models as formation kinetics can be considered to be negligible compared to the other time scales of the flow.

4.1.1 Finite Rate Kinetics

A finite-rate kinetics model for the formation of hydrates (based on interfacial super-saturation) was implemented in TransAT. It is called the Bishnoi model. This model (Vysniauskas & Bishnoi, 1983) is as follows:

$$r = A a_s \exp(-\frac{\Delta E_a}{RT}) \exp(-\frac{a}{\Delta T^b}) \cdot P^\gamma \tag{4.1}$$

with the default values used for the constants listed in Table 4.1.

4.1.2 Instantaneous Kinetics

The instantaneous formation model has been implemented in TransAT as follows.

- Similar to the finite-rate model, the temperature in each cell is compared to the T_{eq} for formation of hydrates. Several curves are available in TransAT for the following materials:

  - Methane
  - Ethane

Constant	Value
A	$4.55 \times 10^{-26} \ \frac{\text{cm}^3}{\text{cm}^2 \, \text{min} \, \text{bar}^\gamma}$
ΔE_a	106204 J/gmol
γ	2.986
a	$0.078 \, \text{K}^\text{b}$
b	2.411

Table 4.1: Hydrates kinetics model (Vysniauskas & Bishnoi, 1983)

- – Propane

- – Isobutane

If the temperature in the computational cell is higher than T_{eq} then no hydrates are formed.

- Note that if the hydrate formation rate is high, then locally more heat will be released resulting in a higher temperature. If the temperature goes higher than T_{eq} then hydrate formation is inhibited. The iterations per time step in the implicit method allow one to obtain the converged solution of the correct temperature and reaction rate.

- The number of moles of hydrate forming phase (hf) in a computational cell is given as:

$$M_{hf} = \frac{\rho_{hf} \alpha_{hf} \Omega_i}{Mw_{hf}} \tag{4.2}$$

where, Mw_{hf} is the molecular weight of hydrate forming phase, M_{hf} is the number of moles of the hydrate forming phase in the cell, and Ω_i is the volume of the computational cell.

- The number of moles of water in the computational cell is given as:

$$M_w = \frac{\rho_w \alpha_w \Omega_i}{Mw_w} \tag{4.3}$$

where Mw_w is the molecular weight of water, and M_w is the number of moles of water available for hydrate formation.

- The rate of formation of hydrates $\dot{r}$ is then given as:

$$\dot{r} = \frac{1}{\Delta t} \min \left(M_{hf}, \frac{M_w}{n_{hy}} \right) \quad [\text{mol/s}] \tag{4.4}$$

where n_{hy} is the hydration number of the hydrate forming phase. The reaction rate is calculated such that all the hydrate forming phase present in a cell is consumed within one time step (provided that the temperature is less than T_{eq}).

- The hydrate formation rate $\dot{r}$ is updated with a relaxation factor β_{hy} in every iteration for a given time step as follows.

$$\dot{r}^{(k+1)} = (1 - \beta_{hy})\dot{r}^{(k)} + \beta_{hy}\dot{r} \quad [\text{mol/s}] \tag{4.5}$$

where $(k+1)$ denotes the current iteration, and (k) denotes the previous iteration. Relaxation is a measure to prevent oscillations in the reaction rate which in turn prevents the convergence of the volume fraction equations. A relaxation factor of 0.4 is used in TransAT.

4.2   Hydrate Dissociation and Melting

4.2.1   Instantaneous Hydrates Dissociation

An instantaneous hydrates dissociation model has been implemented in TransAT.

- The temperature in each cell is compared to the T_{eq} for formation of hydrates. The same curve as for hydrate formation is used. If the temperature in the computational cell is lower than T_{eq} by ΔT_{sh} then hydrates can form, where ΔT_{sh} is the equilibrium range allowed.

- If the temperature in the computational cell is higher than T_{eq} then hydrates dissociate.

- Note that if the hydrate dissociation rate is high, then locally more heat will be absorbed resulting in a lower temperature. If the temperature goes lower than T_{eq} then hydrate dissociation is inhibited. The iterations per time step in the implicit method, allow one to obtain the converged solution of the correct temperature and reaction rate.

- The number of moles of hydrates (M_{hy}) in a computational cell is given as:

$$M_{hy} = \frac{\rho_{hy}\alpha_{hy}\Omega_i}{Mw_{hy}} \tag{4.6}$$

where, Mw_{hy} is the molecular weight of the hydrate phase, M_{hy} is the number of moles of the hydrate forming phase in the cell, and Ω_i is the volume of the computational cell. The rate of dissociation of hydrates $\dot{r}$ is then given as:

$$\dot{r}_{diss} = \frac{1}{\Delta t}(M_{hy}) \quad [\text{mol/s}] \tag{4.7}$$

The reaction rate is calculated such that all the hydrate phase present in a cell is consumed within one time step, provided that the temperature is higher than $T_{eq} + \Delta T_{sh}$.

- The hydrate dissociation rate $\dot{r}$ is updated with a relaxation factor β_{hy} in every iteration for a given time step as follows.

$$\dot{r}_{diss}^{(k+1)} = (1 - \beta_{hy})\dot{r}^{(k)} + \beta_{hy}\dot{r} \quad [\text{mol/s}] \tag{4.8}$$

where $(k+1)$ denotes the current iteration, and (k) denotes the previous iteration. Relaxation is a measure to prevent oscillations in the reaction rate A relaxation factor of 0.4 is used in TransAT.

4.2.2   Heat Absorption

The formation of hydrates is exothermic. The dissociation of hydrates into water and gas phases is endothermic and results in absorption of heat locally. The enthalpy of dissociation is taken to be the same as the enthalpy of formation.

The heat absorbed is included in the mixture temperature equation as a sink term given by,

$$Q_{hy,diss} = \dot{r}_{diss} H_{hy,diss} \, [\text{W}] \tag{4.9}$$

where $H_{hy,diss}$ is the enthalpy of hydrate dissociation, and $\dot{r}_{diss}$ is the rate of dissociation of hydrates. With the dissociation and the related heat absorption, the hydrate volume fraction at any location is a non-linear dynamic balance between possible formation and dissociation (with a gap of $T_{sh} - T_{sc}$ between the formation and dissociation limits for numerical stability).

4.3   Hydrate Rheology

A special hydrate rheology model has been implemented in TransAT.

First, the continuous phase is defined depending on the Water Cut. If it is more than 50%, water is the continuous phase. Otherwise, oil is the continuous phase.

The volume fraction of the dispersed phase is then calculated as follows

$$\alpha_d = \frac{\alpha_{\text{oil}} + \alpha_{\text{water in hydrates}}}{\alpha_{\text{free water}} + \alpha_{\text{oil}} + \alpha_{\text{water in hydrates}}} \quad \text{If water is the continuous phase}$$

$$\tag{4.10}$$

$$\alpha_d = \frac{\alpha_{\text{free water}} + \alpha_{\text{water in hydrates}}}{\alpha_{\text{oil}} + \alpha_{\text{water in hydrates}}} \quad \text{else}$$

where $\alpha_{\text{water in hydrates}} = H\alpha_{\text{hydrates}}$, with H the hydration number. The viscosity of the slurry is then calculated using Mills law (Mills, 1985):

$$\mu_{\text{slurry}} = \mu_{\text{continuous}} \frac{1 - \alpha_{eff}}{\left(1 - \frac{\alpha_{eff}}{\alpha_{max}}\right)^2} \tag{4.11}$$

with

$$\alpha_{eff} = \alpha_d \left(\frac{\tau}{\tau_0}\right)^x \tag{4.12}$$

where τ denotes the instantaneous shear stress. For numerical reasons, in the implementation τ_0 cannot be smaller than 10^{-6} Pa and α_{eff} must not be larger than $0.997\alpha_{max}$.

Bibliography

ANTAL, S. P., LAHEY, R. T. & FLAHERTY, J. E. 1991 Analysis of phase distribution in fully developed laminar bubbly two-phase flow. *Int. J. Multiphase Flow* **17** (5), 635–652.

AUTON, T. R. 1987 The lift force on a spherical body in a rotational flow. *J. Fluid Mech.* **183**, 199–218.

BANERJEE, S., LAKEHAL, D. & FULGOSI, M. 2004 Surface divergence models for scalar exchange between turbulent streams. *International Journal of Multiphase Flow* **30**, 963–977.

BANERJEE, S., RHODES, S. & SCOTT, D. 1968 Mass transfer through falling wavy liquid films in turbulent flows. *Industrial & Engineering Chemistry Fundamentals* **7**, 22.

COSTE, P. 2004 Computational simulation of multi-D liquid-vapor thermal shock with condensation. In *Proceedings of ICMF'04*. Yokohama, Japan.

CROWE, C., SOMMERFELD, M. & TSUJI, Y. 1998 *Multiphase flows with droplets and particles*. Boca Raton, Florida, USA: CRC Press.

DAVIS, J. & YADIGAROGLU, G. 2004 Direct contact condensation in hiemenz flow boundary layers. *Int. J. Heat and Mass Transfer* **47**, 1863–1875.

DE GENNES, P.-G. 1985 Wetting: statics and dynamics. *Reviews of modern physics* **57** (3), 827.

DEIMEL, C., GÜNTHER, M. & SKODA, R. 2014 Application of a pressure based cfd code with mass transfer model based on the rayleigh equation for the numerical simulation of the cavitating flow around a hydrofoil with circular leading edge. In *EPJ Web of Conferences*, , vol. 67, p. 02018. EDP Sciences.

DREW, D. A. & LAHEY, R. T. 1987 The virtual mass and lift force on a sphere in rotating and straining nviscid flow. *Int. J. Multiphase Flow* **13**, 113–121.

DREW, D. A. & PASSMAN, S. L. 1998 *Theory of multicomponent fluids*. Springer-Verlag New York, Inc.

E. KREPPER, B. K. & EGOROV, Y. 2007 Cfd modelling of subcooled boiling concept, validation and application to fuel assembly design. *Nuclear Engineering and Design* **237**, 716–731.

ELGHOBASHI, S. & TRUESDELL, G. C. 1992 Direct simulation of particle dispersion in a decaying isotropic turbulence. *J. Fluid Mech.* **242**, 655–700.

F.M. AUZERAIS, R. J. & RUSSEL, W. 1988 The resolution of shocks and the effects of compresisble sediments in transient settling. *J. Fluid Mech.* **195**, 437.

FRANK, T., SHI, J. M. & BURNS, A. D. 2004 Validation of eulerian multiphase flow models for nuclear safety applications. In *3rd International Symposium on Two-Phase Flow Modelling and Experimentation*. Pisa, Italy.

FRIESS, H. & LAKEHAL, D. 2004 A new method for including interfacial tension and wetting dynamics in the simulation of two-phase flow. In *ICHMT DIGITAL LIBRARY ONLINE*. Begel House Inc.

GYDASPOW, D. 1989 Hydrodymanmics of fluidization and heat transfer supercomputer mmodeling. *Appl. Mech. Rev.* **39**, 1.

HALLANGER, A., SVEBERG, K., ANFINSEN, N., SØNSTABØ, I. & KNUTSEN, T. 1995 A simulation model for three-phase gravity separators. In *2nd Colloquiun on Process Simulation*, pp. 199–213. Helsinki University of Technology, Espoo, Finland.

HARRIS, S. E. & CRIGHTON, D. G. 1994 Solutions, solitary waves and voidage disturbances in gas-fluidized beds. *J. Fluid Mech.* **266**, 243.

HOSOKAWA, S., TOMIYAMA, A., MISAKI, S. & HAMADA, T. 2002 Lateral migration of single bubbles due to the presence of wall. In *In Prococeedings of ASME Joint U.S.European Fluids Engineering Division Conference*. Montreal, Canada.

HUGHES, E. & DUFFEY, R. 1991 Direct contact condensation and momentum transfer in turbulent separated flows. *International Journal of Multiphase Flow* **17**, 599–619.

ISHII, M. 1975 *Thermo-Fluid Dynamic Theory of Two-Phase Flow*. Paris, France: Eyrolles.

ISHII, M. & MISHIMA, K. 1984 Two-fluid model and hydrodynamic constitutive relations. *Nucl. Eng. and Des.* **82**, 107–126.

ISHII, M. & ZUBER, N. 1979 Drag coefficient and relative velocity in bubbly, droplet or particulate lows. *AIChE Journal* **25**, 843.

JOHNSON, P. C. & JACKSON, R. 1987 Frictional-collisional constitutive relations for granular materials, with application to plane shearing. *J. Fluid Mech.* **176**, 64–93.

KOLEV, N. 2002 *Multiphase Flow Dynamics: Mechanical and thermal interactions. Engineering online library* . Springer.

KURUL, N. & PODOWSKI, M. Z. 1991 On the modeling of multidimensional effects in boiling channels. *Proceedings of the 27th National Heat Transfer Conference* pp. 30–40.

LAKEHAL, D., FULGOSI, M., BANERJEE, S. & YADIGAROGLU, G. 2008*a* Turbulence and heat exchange in condensing vapor-liquid flow. *Physics of Fluids* **20**, 065101.

LAKEHAL, D., FULGOSI, M. & YADIGAROGLU, G. 2008*b* DNS of a condensing stratified steam-water flow. *Journal of Heat Transfer* **130**, 02501–10.

LAKEHAL, D. & LABOIS, M. 2011*a* A new modelling strategy for phase-change heat transfer in turbulent interfacial two-phase flow. *Int. J. Multiphase Flow* **37**, 627–639.

LAKEHAL, D. & LABOIS, M. 2011*b* A new modelling strategy for phase-change heat transfer in turbulent interfacial two-phase flow. *International Journal of Multiphase Flow* **37** (6), 627–639.

LAKEHAL, D., MESTAYER, P. G., EDSON, J. B., ANQUETIN, S. & SINI, J.-F. 1995 Eulero-lagrangian simulation of raindrop trajectories and impacts within the urban canopy. *Atmospheric Environment* **29**, 3501–3517.

LIM, I. S., TANKIN, R. S. & YUEN, M. C. 1984 Condensation measurement of horizontal cocurrent steam-water flow. *ASME J. Heat Transfer* **106**, 425–432.

MANNINEN, M. & TAIVASSALO, V. 1996 *On the mixture model for multiphase flow*. Espoo, Finland: VTT Publications.

MAXEY, M. R. & RILEY, J. K. 1983 Equation of motion for a small rigid sphere in a nonuniform flow. *Phys. Fluids* **26**, 883–889.

MILLS, P. 1985 Non-newtonian behaviour of flocculated suspensions. *Journal de Physique – Lettres* **46**, L301–L309.

NARAYANAN, C. & LAKEHAL, D. 2006 Simulation of filling of microfluidic devices using a coarse-grained continuum contact angle model. In *NSTI Nanotechnology Conference and Trade Show*, , vol. 711. Boston.

NARAYANAN, C., LAKEHAL, D. & YADIGAROGLU, G. 2002 Linear stability analysis of particle–laden mixing layers using lagrangian particle tracking. *Powder Tech.* **125**, 122–130.

OESTERL, B. & DINH, T. B. 1998 Experiments on the lift of a spinning sphere in a range of intermediate reynolds numbers. *Experiments in Fluids* **25**, 16–22, 10.1007/s003480050203.

OSHER, S. & SETHIAN, J. A. 1988 Fronts propagating with curvature-dependent speed: Algorithms based on hamilton-jacobi formulations. *J. Comp. Phys.* **79**, 12–49.

QIAN, T., WANG, X.-P. & SHENG, P. 2004 Power-law slip profile of the moving contact line in two-phase immiscible flows. *Physical review letters* **93** (9), 094501.

RANZ, W. E. & MARSHALL, W. R. 1952 Evaporation from drops. *Chemical Engineering Progress* **48** (3), 141–146.

RUBINOW, S. I. & KELLER, J. B. 1961 The transverse force on a spinning sphere moving in a viscous fluid. *Journal of Fluid Mechanics* **11** (03), 447–459.

RZEHAK, R., KREPPER, E. & LIFANTE, C. 2012 Comparative study of wall-force models for the simulation of bubbly flows. *Nucl. Eng. Des.* **253** (0), 41–49.

SCHILLER, L. & NAUMANN, A. Z. 1933 A drag coefficient correlation. *Ver. Deutch Ing.* **77** (0), 318–320.

SINGHAL, A. K., ATHAVALE, M. M., LI, H. & JIANG, Y. 2002 Mathematical basis and validation of the full cavitation model. *Journal of fluids engineering* **124** (3), 617–624.

SNIDER, D. M. 2001 An incompressible three-dimensional multiphase particle-in-cell model for dense particle flows. *Journal of Computational Physics* **170**, 523–549.

SUSSMAN, M., SMEREKA, P. & OSHER, S. 1994 A level set approach for computing solutions to incompressible two-phase flow. *J. Comp. Phys.* **114**, 146–159.

THEOPHANOUS, T., HOUZE, R. & BRUMFIELD, L. 1976 Turbulent mass transfer at free gas-liquid interfaces, with application to open-channel, bubble and jet flow. *International Journal of Multiphase Flow* **19**, 613–623.

TOMIYAMA, A. 1998*a* Drag coefficients of single bubbles under normal and micro gravity conditions **41**, 472–479.

TOMIYAMA, A. 1998*b* Struggle with computational bubble dynamics. In *Proc. of the Third International Conference on Multiphase Flow*. ICMF'98, Lyon, France.

TOMIYAMA, A., SOU, A., ZUN, I., KANAMI, N. & SAKAGUCHI, T. 1995 Effects of eotvos number and dimensionless liquid volumetric flux on lateral motion of a bubble in a laminar duct flow. In *Proceedings of the Second International Conference on Multiphase Flow*, pp. 3–16. Kyoto, Japan.

UBBINK, O. 1997 Numerical prediction of two fluid systems with sharp interfaces. Doctoral thesis, Imperial College London (University of London).

UBBINK, O. & ISSA, R. 1999 A method for capturing sharp fluid interfaces on arbitrary meshes. *Journal of computational physics* **153** (1), 26–50.

VYSKOCIL, L. & MACEK, J. 2008 Boiling flow simulation in neptune cfd and fluent codes. *XCFD4NRS* .

VYSNIAUSKAS, A. & BISHNOI, P. R. 1983 A kinetic study of methane hydrate formation. *Chemical Engineering Science* **38** (7), 1061–1072.

YUAN, W., SAUER, J. & SCHNERR, G. H. 2001 Modeling and computation of unsteady cavitation flows in injection nozzles. *Mécanique & industries* **2** (5), 383–394.